Supporting information

for

Evidence for Tetranuclear bis-*µ*-oxo Cubane Species in Molecular Iridium-based Water Oxidation Catalysts from XAS Analysis

Stuart A. Bartlett,[b,c]* Emma V. Sackville,[a] Emma K. Gibson,[d,e] Veronica Celorrio,[d] Peter P. Wells,[d,f] Maarten Nachtegaal,[g] Stafford W. Sheehan,[h] and Ulrich Hintermair[a]*

a. Centre for Sustainable Chemical Technologies, University of Bath, Bath BA2 7AY, United Kingdom. E-mail: u.hintermair@bath.ac.uk
b. Dynamic Structural Science, Rutherford Appleton Laboratory, Research Complex at Harwell OX11 0FA, United Kingdom. E-mail: stuart.bartlett@sydney.edu.au
c. School of Chemistry, University of Sydney, Sydney NSW 2006, Australia.
d. Rutherford Appleton Laboratory, UK Catalysis Hub, Research Complex at Harwell OX11 0FA, United Kingdom.
e. School of Chemistry, University of Glasgow, Glasgow G12 8QQ, United Kingdom.
f. School of Chemistry, University of Southampton, Southampton SO17 1BJ, United Kingdom.
g. Paul Scherrer Institute, 5232 Villigen, Switzerland.
h. Catalytic Innovations LLC, Fall River, MA 02732, United States.

XAS Fitting analysis of iridium samples

General XAS fitting methodology

All XAS was processed and analysed using the IFEFFIT software (Athena and Artemis).[1] In all analyses the fixed parameters were set as the path coordination number, as determined by the IFEFFIT software, and the amplitude reduction factor set to 0.83, derived from the analysis of the IrO_2 reference. The distance (ΔR), Debye-Waller (σ^2) and E_0 values were set as variables for each shell as indicated in the tables below. ΔR is a fit determined value of the change in distance of the shell from the given model. σ^2 can reasonably be assumed as a wave dampening factor and is typically assumed as the disorder of the shell (i.e. high σ^2 = high damping of wave = high disorder). ΔE_0 is the change in edge shift as determined by the EXAFS analysis. In the main paper, the Fourier Transform EXAFS is plotted with the phase shift added as referenced by the nearest neighbour path (Ir-O), hence $R + \Delta R_{Ir-O}$. In the plots displaying fitting analysis in the supporting information, the phase shift has not been added to the Fourier Transform for clarification of the fit analysis.

Determination of the measure of the accuracy of fitting, R_{fac}

The statistical fitting analysis follows the IFEFFET software and further detail is provided in the published literature.[2] Essentially, a difference function, f, between the data and calculation is computed for each data point included in the evaluation of the fit, where the fit is derived from the sum of the pathways given by the EXAFS equation. The overall statistical verification of the fit as compared with the data is evaluated in the R-space, given by R_{fac}. R_{fac} is evaluated over all data points included in the fit (as defined by the R value given for each analysis). It is interpreted as a numerical evaluation of how closely the fitted function over plots the data. i.e. the smaller the R_{fac} the better the fit. As such it is a useful metric for judging accuracy of the data and the model. It does not define the physical viability of the individual parameters contributing to the fit and thus both R_{fac} and all parameters contributing to that fit must be judged accordingly. The definition of the R_{fac} for the EXAFS analysis is:

$$R_{fac} = \frac{\sum_{i=1}^{N} \left[f(R_i)\right]^2}{\sum_{i=1}^{N} \left(\left[\mathrm{Re}(\tilde{\chi}(R_i|\mathrm{data}))\right]^2 + \left[\mathrm{Im}(\tilde{\chi}(R_i|\mathrm{data}))\right]^2 \right)}$$

Where $f(R_i) = \mathrm{Re}\left[\tilde{\chi}(R_i|\mathrm{data}) - \tilde{\chi}(R_i|\mathrm{theory})\right] + \mathrm{Im}\left[\tilde{\chi}(R_i|\mathrm{data}) - \tilde{\chi}(R_i|\mathrm{theory})\right]$

Where Re = Real Fourier transform, Im = Imaginary Fourier transform, $\tilde{\chi}$ = Fourier Transform EXAFS (determined by the *k*-range); f = difference between the data and calculation for each data point included in the evaluation of the fit.

For a fit evaluated in the R-space, the difference function includes the real and imaginary parts of the Fourier transformed data as given above by $f(R_i)$ (as such imaginary part and [Imaginary + real FT] are shown in each fitting analysis).

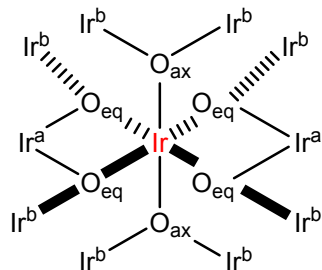## Details of the EXAFS Analyses of the iridium oxide

Figure S1. Structure unit of IrO$_2$ fitted for EXAFS data analysis based on the IrO$_2$ rutile crystal structure. Labels indicative of scattering pathways (below).[3]
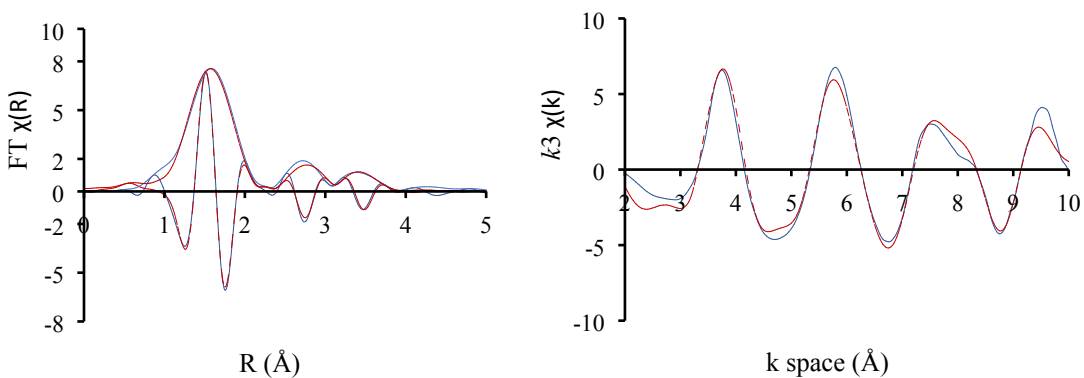

Figure S2. Ir L$_3$ Edge EXAFS experimental (Blue) and fit (red –dashed) data of IrO$_2$ with k^3 weighting. Displaying Fourier transform EXAFS data (Left) and EXAFS plot (Right).

Table S1. Ir L_3 Edge EXAFS fit data of IrO_2 showing fitted pathways, coordination number, distance and fit parameters (numbers in brackets show deviation, indicating variable; MS = multi-scattering pathways).

Paths (with Coordination)	R (Å)	σ^2
6 Ir-O	1.98(1)	0.006(1)
2 Ir-Ir$_a$	3.11(3)	0.006(3)
*28 Ir-O (MS)	3.32 – 3.68(9)	0.007(13)
*58 Ir-O (MS)	3.79 – 4.03(3)	0.009(7)
8 Ir – Ir$_b$	3.52(8)	0.017(11)

E_0 = 12 (2), R-Factor 0.001. $S0^2$ = 0.83 (set). k-range = 2.0– 10; R – range = 1.2 – 4. k-weight = 2,3.

*Predominately multi-scattering pathways. Two separate shells each with one σ^2 and ΔR. The pathways and their amplitude are given below:

28 Ir-O (MS) @ 3.11 – 3.46 Å

Pathway	Degeneracy
Ir-O$_{eq}$-O$_{ax}$-Ir	24
*Ir-O -Ir	4

* Single scattering via O-Ir^b-O$_{eq}$-Ir

28 Ir-O (MS) @ 3.90 – 3.98 Å

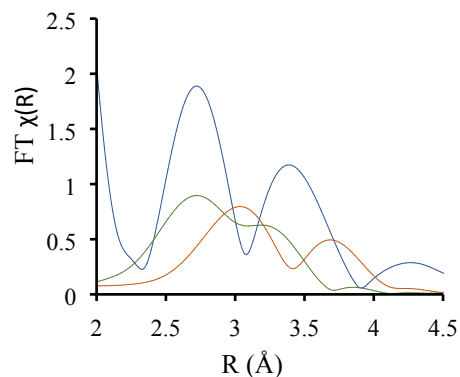| Pathway	Degeneracy
Ir-O$_{ax}$-O$_{ax}$-Ir	2
Ir-O$_{ax}$-Ir-O$_{ax}$-Ir	4
Ir-O$_{ax}$-Ir^b-O$_{ax}$-Ir	4
Ir-O$_{eq}$-Ir^b-O$_{eq}$-Ir	4
Ir-O$_{eq}$-Ir-O$_{ax}$-Ir	16
Ir-O$_{eq}$-O$_{eq}$-Ir	4
Ir-O$_{eq}$-Ir-O$_{eq}$-Ir	8
Ir-Ir-O-Ir	16

Figure S3. Comparison Ir L_3 Edge Fourier transform EXAFS data and fitted Ir-Ir scattering pathways with k^3-weighting (IrO$_2$ experimental EXAFS data = Blue; 2 Ir-Ir {3.11 Å} = Green; 8 Ir-Ir {3.52 Å} = Orange).
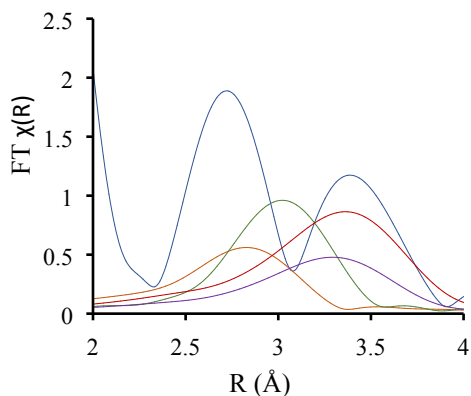

Figure S4. Comparison Ir L_3 Edge Fourier transform EXAFS data and fitted Ir-O scattering pathways (only major contributions shown) with k^3-weighting (IrO$_2$ experimental EXAFS data = Blue; 24 Ir-O$_{ax}$-O$_{eq}$-Ir {3.48 Å} = Orange; Ir-O -Ir {3.51 Å} = Green; Ir-O$_{ax}$-Ir-O$_{ax}$-Ir {3.95 Å} = Purple; Ir-O$_{eq}$-Ir-O$_{eq}$-Ir {4.03 Å} = Red)

XAS fitting analysis of Ir-WOC dimer model (2):

Table S2. Ir L_3 Edge EXAFS fit data of Ir-Blue showing fitted pathways, coordination number, distance and fit parameters for dimer model (numbers in brackets show deviation, indicating variable; MS = multi-scattering pathways).

Paths (with Coordination)	Distance (Å)	Debye-Waller
2 Ir-O	1.96(1)	0.002(1)
4 Ir-O/N	2.50(7)	0.012(13)
1 Ir – Ir	2.97(4)	0.002(3)
26 Ir-O MS	3.1 – 3.3 (1)	0.005(17)
40 Ir-O MS	3.89 – 4.01 (7)	0.001(8)

E_0 = 8.6(3), R-Factor 0.006. Amp = 0.83 (set). k-range = 2.7 – 12 R – range = 1.2 – 4. k-weight = 2,3.

28 Ir-O (MS) @ 3.2 – 3.5 Å

Pathway	Degeneracy
Ir-Ir-O-Ir	4
Ir-O-O-Ir	22

28 Ir-O (MS) @ 3.91 – 4.01 Å

Pathway	Degeneracy
Ir-O-Ir-O-Ir	34
Ir-O-O-Ir	6

XAS fitting analysis of Ir-WOC cubane model (3):

Table S3. Ir L_3 Edge EXAFS fit data of Ir-WOC showing fitted pathways, coordination number, distance and fit parameters for cubane model (numbers in brackets show deviation, indicating variable; MS = multi-scattering pathways).

Paths (with Coordination)	Distance (Å)	Debye-Waller
3 Ir-O	1.96(3)	0.006(4)
3 Ir-O/N	2.04(3)	0.001(1)
3 Ir – Ir	2.97(3)	0.012(3)
30 Ir-O MS	3.22 – 3.58 (9)	0.010(16)
39 Ir-O MS	3.91 – 4.01 (5)	0.008(6)

E_0 = 8.6(1), R-Factor 0.001. Amp = 0.83 (set). k-range = 2.7 – 12; R – range = 1.2 – 4. k-weight = 2,3.

30 Ir-O (MS) @ 3.22 – 3.58 Å

Pathway	Degeneracy
Ir-Ir-O-Ir	12
Ir-O-O-Ir	18

39 Ir-O (MS) @ 3.91 – 4.01 Å

Pathway	Degeneracy
Ir-O-Ir-O-Ir	27
Ir-O-Ir-O-Ir	6
Ir-O-O-Ir	6

XAS fitting analysis of Ir-WOC mono-oxo dimer model (1)

A mono-oxo dimer has previously been suggested.[4] Using the published structure derived from the given DFT Cartesian coordinates, we compare our EXAFS data with that model with the given EXAFS fit parameters as published in Bastia *et al*. for the activated catalyst.[4] The Ir L_3 Edge EXAFS experimental Ir-Blue and mono-oxo bridged dimer fit data with k^3 weighting (displayed in Figure 4 in the main article) resulted in an R-factor = 0.014 with ΔE_0 = 14.5 eV when compared with our data set.

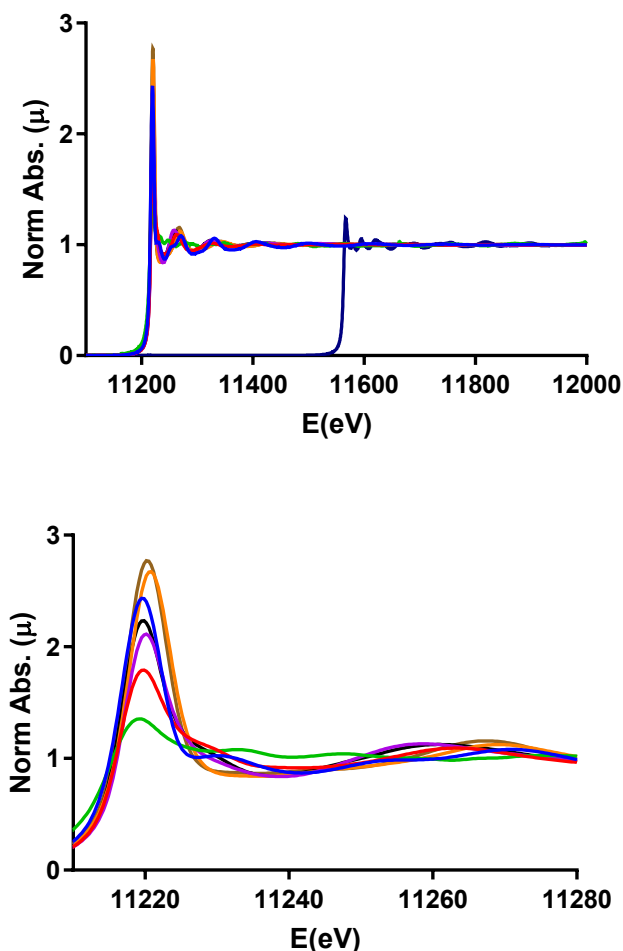## Ir L_3-edge XANES comparison of Ir samples and Pt foil reference

Figure S5. Displaying normalised XANES spectra as calibrated to the platinum foil L_3-edge and magnification of Iridium L_3 edge with associated edge energies taken as the first derivative of the absorption edge (Samples = $Na_2Ir^{IV}Cl_6$ (11216 eV); $[Ir^I(cod)Cl]_2$ (11217 eV); Ir^0 foil (11214 eV); $[Cp*Ir^{III}(H_2O)_3]SO_4$ (11216 eV); $Ir^{IV}O_2$ (11217 eV); $[Cp*Ir^{III}(pyalk)Cl]$ (11217 eV); Ir-WOC (11216 eV); Pt-Foil (11564 eV - top only).
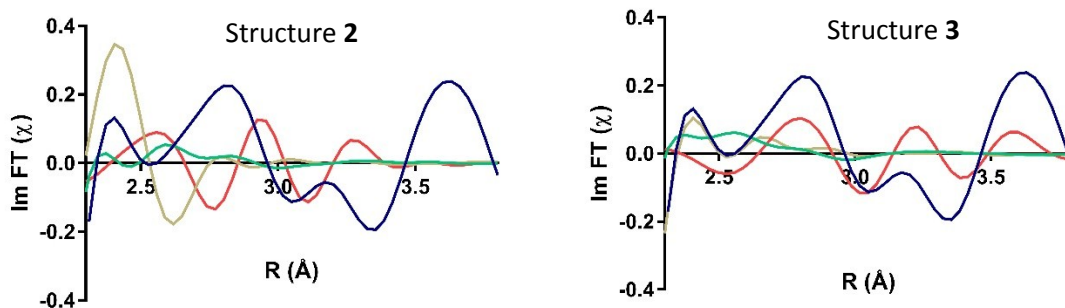
Figure S6. Plots showing the k^3 weighted imaginary components of the Fourier transform of the experimental EXAFS data (blue), Ir-Ir shell (red), bridging O atoms (green) and Ir-O/N pyalk ligand shell (yellow) for structure **2** (left) and **3** (right) respectively.

References

1. B. Ravel, M. Newville, ATHENA, ARTEMIS, HEPHAESTUS: data analysis for X-ray absorption spectroscopy using IFEFFIT, *Journal of Synchrotron Radiation* **12**, 537–541 (2005).
2. B. Ravel, "Quantitative EXAFS analysis," in *X-Ray Absorption and X-Ray Emission Spectroscopy: Theory and Applications*, edited by J. A. van Bokhoven and C. Lamberti (John Wiley & Sons, Ltd., Chichester, UK, 2016), pp. 281–302.
3. Bolzan, A. A.; Fong, C.; Kennedy, B. J.; Howard, C. J., Structural Studies of Rutile-Type Metal Dioxides, *Acta Crystallographica Section B*, **B(53)**, 373-380. (1997).
4. Yang, K. R.; Matula, A. J.; Kwon, G.; Hong, J.; Sheehan, S. W.; Thomsen, J. M.; Brudvig, G. W.; Crabtree, R. H.; Tiede, D. M.; Chen, L. X.; Batista, V. S., Solution Structures of Highly Active Molecular Ir Water-Oxidation Catalysts from Density Functional Theory Combined with High-Energy X-ray Scattering and EXAFS Spectroscopy. *Journal of the American Chemical Society*, *138* (17), 5511-5514 (2016).